Available online at www.sciencedirect.com
ScienceDirect
Trans. Nonferrous Met. Soc. China 25(2015) 4110−4118
Transactions of Nonferrous Metals Society of China
www.tnmsc.cn

Sulfur composition on surface of chalcopyrite during its bioleaching at 50 °C

Shi-fa WU, Cong-ren YANG, Wen-qing QIN, Fen JIAO, Jun WANG, Yan-sheng ZHANG

School of Minerals Processing and Bioengineering, Central South University, Changsha 410083, China

Received 2 February 2015; accepted 25 August 2015

Abstract: The composition of passive layer of chalcopyrite was investigated by X-ray photoelectron spectroscopy (XPS), accompanied with cyclic voltammetry (CV). The leaching experiment shows that the extraction rates of Cu with leaching for 30 d by sterile control and microorganisms are 4.0% and 21.5%, respectively. In comparison, 3.8% and 10.5% Fe are leached by sterile control and microorganisms, respectively. The results of XPS studies suggest that Fe atoms dissolve preferentially from the chalcopyrite lattice, and disulfide (S_2^{2-}), polysulfide (S_n^{2-}) and elemental sulfur (S^0) are identified on the chalcopyrite surfaces leached by sterile control and microorganisms. Additionally, sulfate (SO_4^{2-}) is detected on the chalcopyrite surfaces leached by microorganisms, and most of it probably originates from jarosite. The analysis of CV results reveals that metal-deficient sulfide ($Cu_{1-x}Fe_{1-y}S_{2-z}$, $y>x$) and elemental sulfur (S^0) passivate the surface of chalcopyrite electrode. The elemental sulfur and/or jarosite coating on the chalcopyrite surface may have impact on the leaching process; however, the disulfide, polysulfide or metal-deficient sulfide plays a more key role in the chalcopyrite leaching.

Key words: bioleaching; chalcopyrite; passive layer; electrochemistry

1 Introduction

Chalcopyrite is the main source of copper in the world [1−3]. More than 80% copper is available as chalcopyrite, and around 20% copper in the world is obtained through hydrometallurgical process [3]. Much attention has also been paid to the bioleaching of chalcopyrite [4−8]. The mesophiles (30−40 °C), moderate thermophiles (about 50 °C) and extreme thermophiles (>65 °C) microbes are usually used to oxidize or assist in the oxidation of chalcopyrite, and such microbes are able to oxidize Fe^{2+} and/or S [1]. Moreover, it has generally been found that the use of moderate thermophiles and thermophiles are beneficial for chalcopyrite leaching [9−11]. Many researchers further suggested that there was clear benefit in leaching chalcopyrite within low solution potential, compared with high potential leaching [11−13].

The chalcopyrite is recalcitrant to both chemical and biological leaching due to the passivation of the mineral surface [6,14], and the passivation layer of chalcopyrite may be affected by leaching conditions such as the pH value and redox potential. Elemental sulfur [15−17], disulfide [15,16,18,19] polysulfide [16,18,20] and jarosite [16,17,21−23] identified on chalcopyrite surfaces leached by chemicals or microorganisms, have all been proposed as passivation candidates. KLAUBER et al [15,16] reported that the main species formed on the chalcopyrite surface are S^0 and S_2^{2-}. ACRES et al [18] identified that there was 16% S_2^{2-} and 43% S_n^{2-}on the surface of chalcopyrite leached in HCl solution for 2 h with the pH value of 1. ZHU et al [21] and HE et al [22] suggested that the jarosite might be the major component of the passivation layer of the chalcopyrite leached by thermophilic archaea.

Hence, it needs to further understand the component of a passivation layer of chalcopyrite bioleaching for successful industrial bioleaching implementation. The objective of the research was to investigate the sulfur speciation during chalcopyrite leaching at 50 °C.

Foundation item: Project (51274255) supported by the National Natural Science Foundation of China; Project (20130162110007) supported by the Doctoral Fund of Ministry of Education of China; Project supported by the Co-Innovation Center for Clean and Efficient Utilization of Strategic Metal Mineral Resources, China

Corresponding author: Cong-ren YANG; Tel: +86-13874962836; E-mail: yangcongren@csu.edu.cn

DOI: 10.1016/S1003-6326(15)64062-6

2 Experimental

2.1 Chalcopyrite

The high grade chalcopyrite was obtained from Daye, Hubei Province, China. The samples were splintered into small fragments with a geological hammer and dry ground in a porcelain ball mill. The product size was screened to less than 0.074 mm for bioleaching experiments. The chemical analysis of the sample shows 33.91% Cu, 30.62% Fe, 32.90% S, 0.039% Pb and 0.018% Zn (mass fraction). The X-ray diffraction analysis of the sample shows that the mineral is chalcopyrite.

2.2 Enrichment culture

A mixed moderately thermophilic culture was enrichment cultured from a leaching solution sample, which was obtained from Inner Mongolia, China, in 250 mL shake flasks using an orbital incubator with a stirring speed of 160 r/min at 50 °C. The medium used for cell cultivation consisted of the following components [24]: 3.0 g/L $(NH_4)_2SO_4$, 0.1 g/L KCl, 0.5 g/L $MgSO_4·7H_2O$, 0.5 g/L K_2HPO_4, 0.01 g/L $Ca(NO_3)_2$ and 0.02% yeast extract. All the cultures were sub-cultured into basal salts medium supplemented with 2% ore powder as the energy source. The resulting mixed culture was used as inoculums for all experiments. Three species (*Sulfobacillus thermosulfidooxidans*, *Acidithiobacillus caldus*, *Ferroplasma sp.*) were detected by community structure analysis as described by QIN et al [25].

2.3 (Bio)leaching experiments

For leaching experiments, the cells were inoculated into 250 mL flasks containing 100 mL sterilized culture medium and 2 g chalcopyrite. The initial cells concentration was 1.0×10^7 cell/mL. The flasks were placed in an orbital shaker at 50 °C with a stirring speed of 160 r/min. The parallel experiments without cells, but with the same culture medium and chalcopyrite, were run as the sterile experiments. All leaching experiments were supplemented with 0.02% yeast extract. The solution pH value was controlled at 1.6−2.0 with diluted sulfuric acid. Water lost by evaporation was supplemented periodically by adding sterile water until the mass of the flask equaled its initial mass.

2.4 Electrochemical measurements

Massive electrodes were prepared by cutting a high quality natural chalcopyrite sample into approximately cylinder shapes with areas of 1 cm^2 exposed to the solution. Before every electrochemical experiment, the working electrode surface was polished with carbide papers from 800 to 3000 grit, and then rinsed with deionized water.

Electrochemical experiments were carried out using a conventional three-electrode electrolytic cell with a graphite rod as the counter electrode and the prepared chalcopyrite electrode as the working electrode. A saturated Ag/AgCl electrode was used as the reference electrode for all the electrochemical tests. Electrochemical response was measured on a Princeton Model 283 potentiostat (EG&G of Princeton Applied Research) coupled to a personal computer with the M270 software. The electrolyte solution was prepared as follows: 3.0 g/L $(NH_4)_2SO_4$, 0.1 g/L KCl, 0.5 g/L $MgSO_4·7H_2O$, 0.5 g/L K_2HPO_4, 0.01 g/L $Ca(NO_3)_2$ with the pH value of 1.6. All the electrochemical experiments were performed at 50 °C in the electrolyte solution.

2.5 Analytical techniques

The mineralogical compositions of solid samples were examined by X-ray diffraction (XRD) (Rigaku D/max−2000). Solubles Cu and Fe were determined by atomic absorption spectroscopy (AAS). The pH value of the supernatant was measured with a pH meter (BPP−922, BELL) and the redox potentials in the leaching solution were measured with a Pt electrode with reference to a saturated Ag/AgCl electrode.

XPS was conducted with an ESCALAB 250Xi spectrometer with a monochromatic Al excitation (1486.6 eV) operating at 200 W. High resolution core level spectra were collected using a pass energy of 20 eV and an energy step of 0.1 eV. The chamber pressure was set to the limit of 1×10^{-7} Pa. The binding energy calibration was based on C 1s at 284.6 eV.

3 Results and discussion

3.1 (Bio)leaching characteristics of chalcopyrite

Figure 1(a) shows that the extraction rates of Cu for the leaching by sterile control and microorganisms for 30 d are 4.0% and 21.5%, respectively. In comparison, the Fe extraction rates are lower than those of Cu, only 3.8% and 10.5% Fe are leached by sterile control and microorganisms (Fig. 1(b)), respectively. The Fe extraction rate decreases due to the precipitation of the soluble ferric iron as the jarosite during bioleaching (Eq. (1)) [11,26]. Figure 1(c) shows that the acid is consumed in the whole leaching process. The redox potential of leaching with the microorganisms reaches and stabilizes at about 630 mV due to ferrous ions being oxidized to ferric ions by the microorganisms, while the redox potential of leaching by sterile control stabilizes at about 370 mV (Fig. 1(d)).

$$M^+ + 3Fe^{3+} + 2SO_4^{2-} + 6H_2O \rightarrow MFe_3(SO_4)_2(OH)_6 + 6H^+ \quad (1)$$

where M is a monovalent cation, e.g., H_3O^+, Na^+, K^+ and NH_4^+.

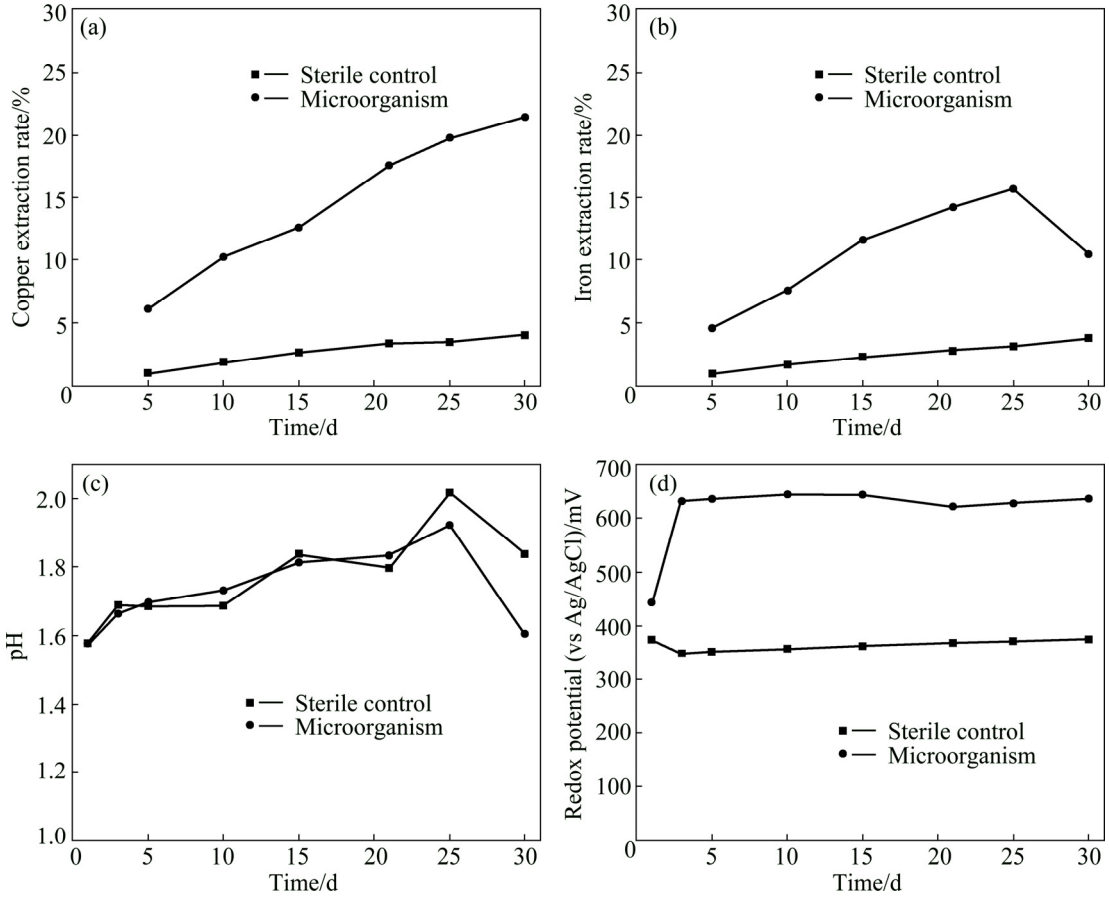

Fig. 1 Copper extraction (a), iron extraction (b), pH value (c) and redox potentials (d) in leach liquors during (bio)leaching of chalcopyrite

In the previous study [11], the authors showed that the extraction rate of Cu for bioleaching of chalcopyrite by a mixed moderately thermophilic culture under the similar conditions was 92.5%, and concluded that the chalcopyrite dissolution rate depended on the redox potential of the solution. Similarly, HIROYOSHI et al [27] found that the leaching rate was significantly enhanced by the addition of 0.50 mol/L Fe^{2+} and 0.01 mol/L Cu^{2+} together with 0.03 mol/L Fe^{3+}. SANDSTRÖM et al [28] suggested that in sulfuric acid media, a low redox potential (620 mV (vs SHE)) was beneficial to chalcopyrite leaching when compared with a higher redox potential (800 mV (vs SHE)). In order to understand this phenomenon, HIROYOSHI et al [27] and GU et al [12] proposed a two-step reaction model for chalcopyrite leaching at low redox potential. Firstly, chalcopyrite is reduced by ferrous to form chalcocite, and then the formed chalcocite is oxidized by ferric. Electrochemical studies have shown that chalcocite might be a possible intermediate compound [12,29,30]. GU et al [12] reported that chalcopyrite was reduced to chalcocite at a low redox potential locating at initial 8 d of bioleaching process, but no reduced product was detected at a high redox potential of about 550 mV (vs SCE). Thus, the dissolution of chalcopyrite would be favored when the redox potential was less than 450 mV (vs Ag/AgCl), or at an appropriate ratio of $n(Fe^{3+})/n(Fe^{2+})$ [11,12,27,28,31,32].

3.2 XRD and XPS analyses of chalcopyrite and leaching residues

Figure 2 shows the XRD patterns of chalcopyrite and residues leached by sterile control and microorganisms. It can be seen that the peaks of tetragonal chalcopyrite are identified. Less amounts of jarosite forms during the bioleaching (Fig. 2(c)).

In order to further investigate the composition of leaching residues, the chalcopyrite and leaching residues were analyzed using XPS. Figures 3(a)−(c) show the S 2p core level peaks. The S 2p peaks also occur as doublets, S $2p_{3/2}$ and S $2p_{1/2}$, as a result of spin–orbit splitting. The S 2p spectra are fitted using a 2:1 peak area ratio for S $2p_{3/2}$ to S $2p_{1/2}$ and 1.2 eV splitting. The peaks fitted to the spectra use a summed Gaussian−Lorentzian (SGL) function to describe the convoluted Gaussian−Lorentzian line shapes of the peaks. The weighting used was 70% Gaussian and 30% Lorentzian. The background of the spectrum was obtained using the Shirley method.

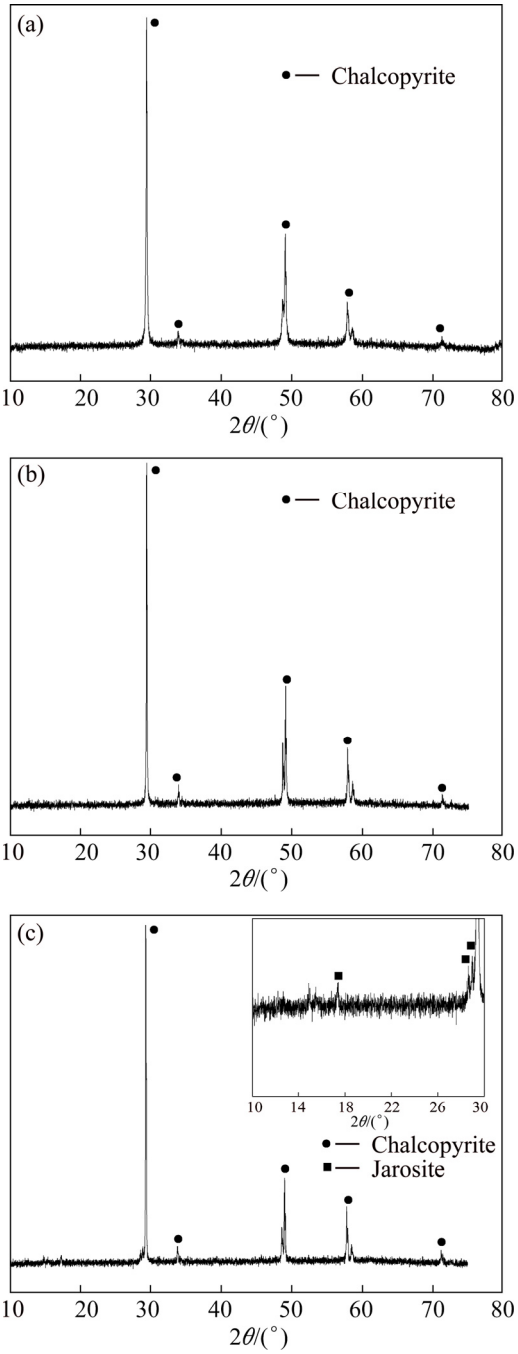

Fig. 2 XRD patterns of chalcopyrite (a), and residues leached by sterile control (b) and microorganisms (c)

Figure 3(a) shows the S 2p core level peaks of chalcopyrite which consist of three major doublets, and the S $2p_{3/2}$ peaks of three doublets in Fig. 3(a) center at 161.3, 161.9 and 162.8 eV, respectively. It was reported that the S $2p_{3/2}$ peak originating from chalcopyrite, i.e. monosulfide (S^{2-}), centers at about 161.4 eV [20,33]. The low intensity S $2p_{3/2}$ peaks centered at 161.9 and 162.8 eV are assigned to S_2^{2-} [18,34] and S_n^{2-} [18,35], respectively. Many authors claimed that the S_2^{2-} species rapidly form a layer on freshly fractured chalcopyrite surfaces [15,18,19,34]. In recently, de OLIVEIRA

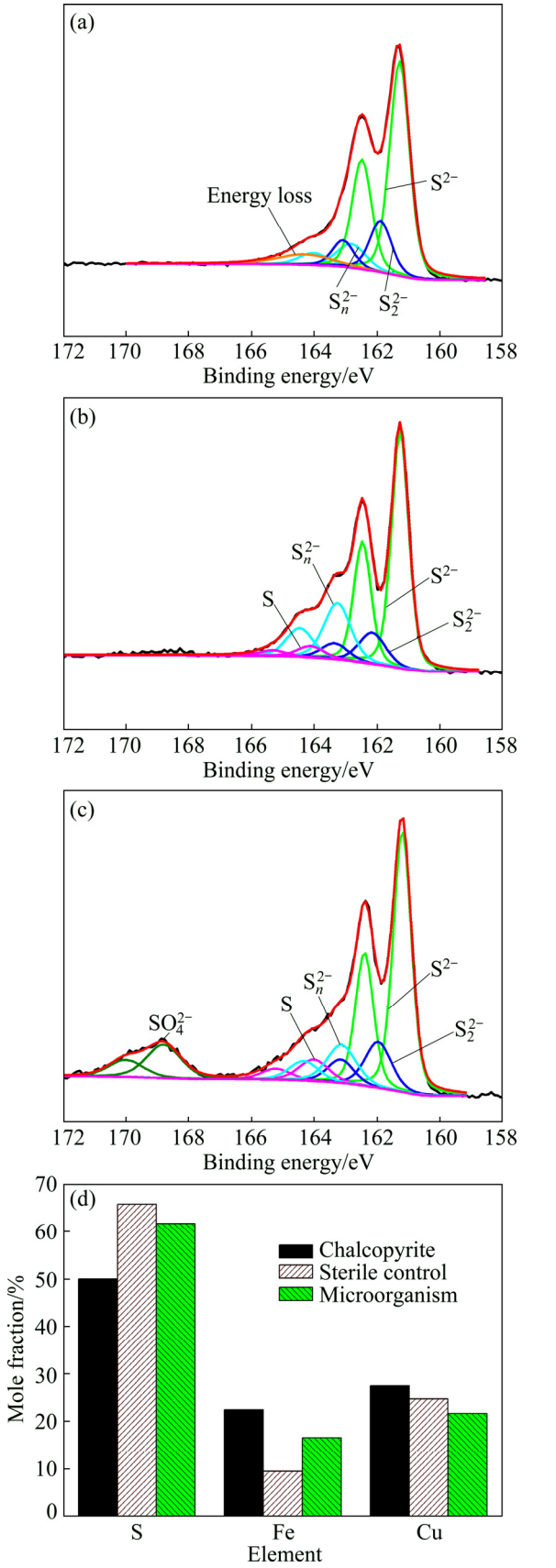

Fig. 3 XPS spectra of S 2p peaks of chalcopyrite exposed to air for no more than a few minutes (a), leached by sterile control (b) and microorganisms (c), and composition of Cu, Fe and S on surface of chalcopyrite before and after leaching (d)

et al [3,36] applied the DFT/plane waves methodology to study the surface of chalcopyrite reconstruction. The results showed the formation of S_2^{2-} and S_4^{2-} on the chalcopyrite surfaces. In addition, a low intensity 2p peak component was obtained at 164.3 eV, which was related to the energy-loss satellite due to the S 3p→Fe 3d excitation [18,34].

Figure 3(b) shows a high-resolution spectrum of S 2p for chalcopyrite leached by sterile control. Four fitting peaks center at 161.3, 162.2, 163.3 and 164.1 eV, arising from the monosulfide [20,23,33,37,38], disulfide [18,35,38], polysulfide [18,23,35] and sulfur [1,23,39,40], respectively. Figure 3(c) shows a high-resolution spectrum of S 2p for chalcopyrite leached by microorganisms. Five fitting peaks center at 161.2, 162.0, 163.1, 164.0 and 168.8 eV, arising from the monosulfide [20,23,33,37,38], disulfide [18,35,38], polysulfide [18,23,35], sulfur [1,23,39,40] and sulfate [1,15,38], respectively, most of which probably originate from jarosite. The formation of S_2^{2-} and S_n^{2-} is due to the dissolution of Cu and Fe atoms from the crystal lattice of chalcopyrite, especially, Fe atoms dissolve preferentially from the chalcopyrite lattice (Fig. 3(d)), and this result is in agreement with the previous works [20,41].

Figure 4(a) shows high-resolution spectra of Cu 2p for original chalcopyrite and residues leached by sterile control and microorganisms. The fitting results of peaks reveal that the Cu $2p_{3/2}$ peak of three samples is in the binding energy range of 932.0 to 932.2 eV, this value is close to the binding energy for the Cu $2p_{3/2}$ in chalcopyrite [33,37,42]. It is worth mentioning that the presence of Cu^{2+} usually results in the appearance of satellite peak around the binding energy of 942 eV [20,43,44]. Since the satellite peak is absent in the Cu 2p core level peaks in Fig. 4(a), cupric is absent on the mineral surface even after being leached by microorganisms.

The high-resolution spectra of Fe 2p for chalcopyrite exposed to air for no more than a few minutes, leached by sterile control and microorganisms are provided in Fig. 4(b). The Fe 2p spectrum shows that the chalcopyrite exposed to air for only a few minutes is oxidized. The peak near 708 eV can be assigned to Fe—S [20]. The peaks in the binding energy range of 710 to 712 eV can be assigned to Fe(III)—O, —OH or —OOH [18,20,23,42]. For the bioleached Fe 2p spectrum, the component near 712 eV binding energy can be assigned to jarosite.

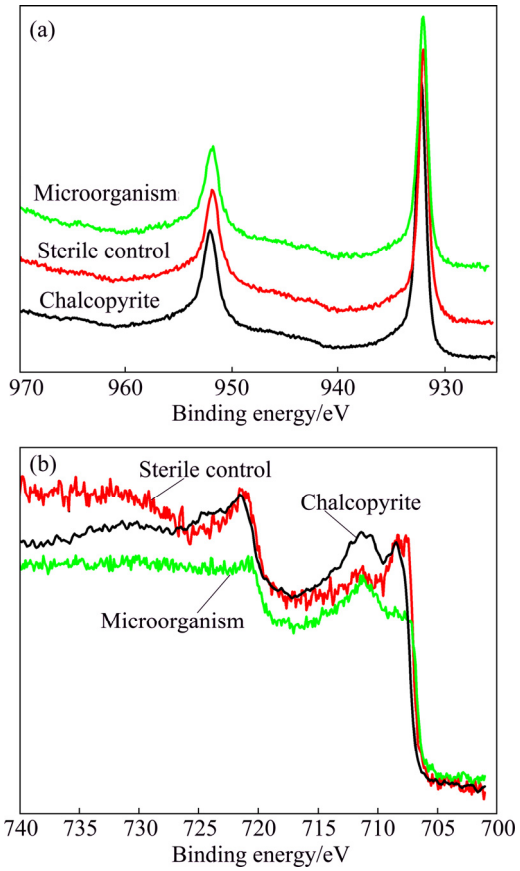

Fig. 4 XPS spectra of Cu 2p peak (a) and Fe 2p peak (b) of chalcopyrite exposed to air for no more than a few minutes, leached by sterile control and microorganisms

3.3 Cyclic voltammetry

Figure 5(a) shows the cyclic voltammograms of massive chalcopyrite electrodes. The potential of the electrode was initially swept from the open circuit potential (OCP) (475 mV) in a positive-going direction with a scan rate of 20 mV/s. The peak A1 is related to the selective dissolution of iron from the chalcopyrite lattice according to Eq. (2) [45,46]. The peak A2 should be assigned to the massive dissolution of chalcopyrite to copper ions, elemental sulfur and/or sulfate [46−48], as shown in Eqs. (3) and (4). The explanation of other peaks is irrelevant to the direct dissolution and passivation of chalcopyrite and not of interest in this study.

$$CuFeS_2 \rightarrow Cu_{1-x}Fe_{1-y}S_{2-z} + xCu^{2+} + yFe^{2+} + zS^0 + 2(x+y)e\ ,\ (y>x) \quad (2)$$

$$CuFeS_2 \rightarrow Cu^{2+} + 2S^0 + Fe^{3+} + 5e \quad (3)$$

$$CuFeS_2 + 8H_2O \rightarrow Cu^{2+} + Fe^{3+} + 2SO_4^{2-} + 16H^+ + 17e \quad (4)$$

Figure 5(b) shows that the anodic oxidation current decreases from 0.74 to 0.66 mA, with increasing the potential from 710 to 800 mV, which indicates that the product of chalcopyrite dissolution in the potential range of 520 to 710 mV accumulates on the surface, and passivates the electrode surface.

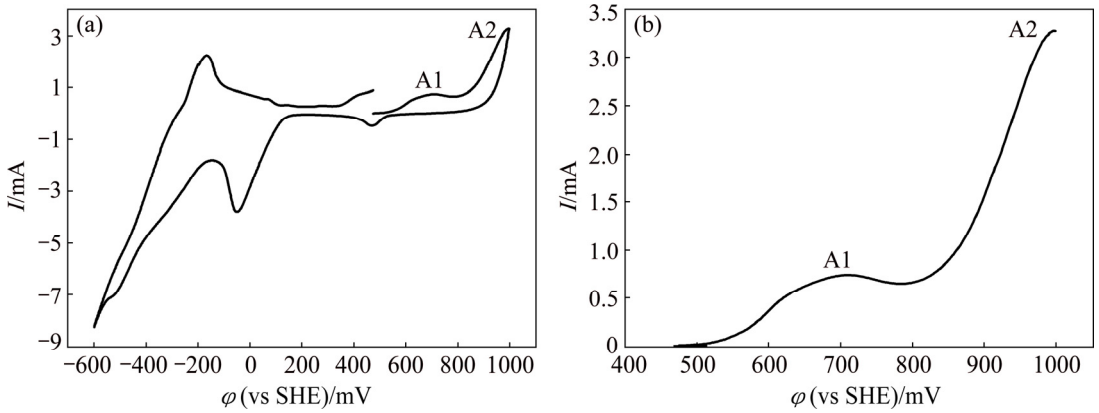

Fig. 5 Cyclic voltammograms (a) and cyclic voltammogram focusing on peaks A1 and A2 (b) of chalcopyrite electrode

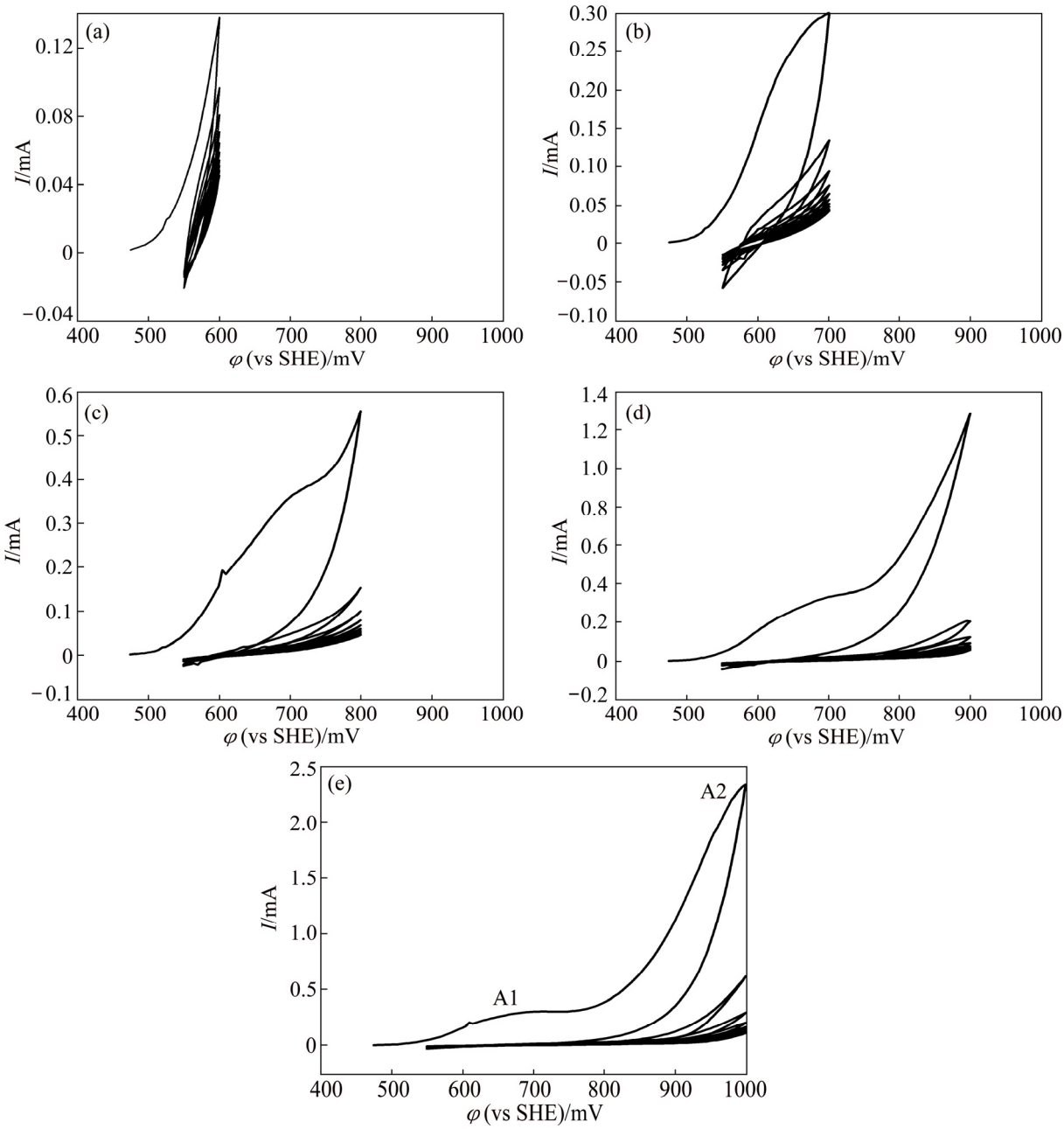

Fig. 6 Multi-cyclic voltammograms (10 cycles) of chalcopyrite electrode with scan rate of 20 mV/s in different potential ranges: (a) 475−600 mV; (b) 475−700 mV; (c) 475−800 mV; (d) 475−900 mV; (e) 475−1000 mV

Figure 6 shows the multi-cyclic voltammograms (10 cycles) of the chalcopyrite electrode in the potential window of 475 to 1000 mV. The electrodes were initially swept from 475 mV to 600, 700, 800, 900 and 1000 mV, respectively, and then swept from 550 mV in the following 9 cycles. Figure 6 shows that the anodic oxidation current decreases with increasing the number of cycles, which indicates that the product of chalcopyrite dissolution accumulates on the surface, and passivates the electrode surface. Figures 5 and 6 also show that the passive film formed in the potential window of 475 to 700 mV will be oxidized when the sweeping potential is above 800 mV.

ZHU et al [21] and HE et al [22] suggested that jarosite might be the major component of the passivation layer of chalcopyrite leached by thermophilic archaea. However, D'HUGUES et al [49] did not find any evidence of jarosite hindrance to leaching chalcopyrite with extreme thermophiles at 78 °C. GU et al [12] reported that the jarosite formed on the chalcopyrite surface was porous and loose, therefore, it cannot be an effective component of a passivation layer to hinder the copper extraction [12]. In the previous study [11], the XRD analysis indicated that a significant amount of elemental sulfur and jarosite formed on the chalcopyrite surface after bioleaching, but the extraction fraction of Cu reached 92.5%. KLAUBER et al [15] found that the main candidates for passivation layer were S^0 and S_2^{2-}. ACRES et al [18] identified 16% S_2^{2-} and 43% S_n^{2-} on the surface of chalcopyrite leached in HCl solution for 2 h with the pH value of 1. MIKHLIN et al [2] identified the presence of S_3^{2-} and S_4^{2-} on the surface of chalcopyrite after the leaching. The results of electrochemical and XPS studies by GHAHRE-MANINEZHAD et al [20] have suggested that a metal-deficient sulfide film passivated the surface of chalcopyrite electrode. MAJUSTE et al [50] suggestesd that the $Cu_{1-x}Fe_{1-y}S_{2-z}$, Cu_5FeS_4 and CuS hindered the electrochemical dissolution of chalcopyrite. S^0 was also detected on the chalcopyrite surfaces, but had no impact on the chalcopyrite dissolution [21,50]. Therefore, the disulfide (S_2^{2-}), polysulfide (S_n^{2-}) or metal-deficient sulfide ($Cu_{1-x}Fe_{1-y}S_{2-z}$) plays a more key role in the chalcopyrite leaching.

4 Conclusions

1) Fe atoms dissolve preferentially from the chalcopyrite lattice. Disulfide, polysulfide and elemental sulfur are identified on the chalcopyrite surfaces leached by sterile control and microorganisms. Additionally, sulfate is detected on the chalcopyrite surfaces leached by microorganisms, and most of sulfate probably originated from jarosite.

2) The metal-deficient sulfide and elemental sulfur passivate the surface of chalcopyrite electrode.

3) The elemental sulfur and/or jarosite coating on the chalcopyrite surface may have impact on the leaching process. However, the disulfide, polysulfide or metal-deficient sulfide plays a more key role in the chalcopyrite leaching.

References

[1] LI Y, KAWASHIMA N, LI J, CHANDRA A P, GERSON A R. A review of the structure, and fundamental mechanisms and kinetics of the leaching of chalcopyrite [J]. Advances in Colloid and Interface Science, 2013, 197: 1−32.

[2] MIKHLIN Y L, TOMASHEVICH Y V, ASANOV I P, OKOTRUB A V, VARNEK V A, VYALIKH D V. Spectroscopic and electrochemical characterization of the surface layers of chalcopyrite ($CuFeS_2$) reacted in acidic solutions [J]. Applications of Surface Science, 2004, 225(1−4): 395−409.

[3] de OLIVEIRA C, de LIMA G F, de ABREU H A, DUARTE H A. Reconstruction of the chalcopyrite surfaces—A DFT study [J]. Journal of Physical Chemistry C, 2012, 116(10): 6357−6366.

[4] CHEN Ming-lian, ZHANG Lin, GU Guo-hua, HU Yue-hua, SU Li-jun. Effects of microorganisms on surface properties of chalcopyrite and bioleaching [J]. Transactions of Nonferrous Metals Society of China, 2008, 18(6): 1421−1426.

[5] ZHU Wei, XIA Jin-lan, PENG An-an, NIE Zhen-yuan, QIU Guan-zhou. Characterization of apparent sulfur oxidation activity of thermophilic archaea in bioleaching of chalcopyrite [J]. Transactions of Nonferrous Metals Society of China, 2013, 23(8): 2383−2388.

[6] GU Guo-hua, HU Ke-ting, LI Shuang-ke. Surface characterization of chalcopyrite interacting with *Leptospirillum ferriphilum* [J]. Transactions of Nonferrous Metals Society of China, 2014, 24(6): 1898−1904.

[7] LIANG Chang-li, XIA Jin-lan, NIE Zhen-yuan, YU Shui-jing, XU Bao-quan. Effect of initial pH on chalcopyrite oxidation dissolution in the presence of extreme thermophile *Acidianus manzaensis* [J]. Transactions of Nonferrous Metals Society of China, 2014, 24(6): 1890−1897.

[8] YU Run-lan, LIU Jing, CHEN An, ZHONG Dai-li, LI Qian, QIN Wen-qing, QIU Guan-zhou, GU Guo-hua. Interaction mechanism of Cu^{2+}, Fe^{3+} ions and extracellular polymeric substances during bioleaching chalcopyrite by *Acidithiobacillus ferrooxidans* ATCC2370 [J]. Transactions of Nonferrous Metals Society of China, 2013, 23(1): 231−236.

[9] BRIERLEY J A, BRIERLEY C L. Present and future commercial applications of biohydrometallurgy [J]. Hydrometallurgy, 2001, 59(2−3): 233−239.

[10] MORIN D, PINCHES T, HUISMAN J, FRIAS C, NORBERG A, FORSSBERG E. Progress after three years of BioMinE—Research and technological development project for a global assessment of biohydrometallurgical processes applied to European non-ferrous metal resources [J]. Hydrometallurgy, 2008, 94(1−4): 58−68.

[11] QIN Wen-qing, YANG Cong-ren, LAI Shao-shi, WANG Jun, LIU Kai, ZHANG Bo. Bioleaching of chalcopyrite by moderately thermophilic microorganisms [J]. Bioresource Technology, 2013, 129: 200−208.

[12] GU Guo-hua, HU Ke-ting, ZHANG Xun, XIONG Xian-xue, YANG Hui-sha. The stepwise dissolution of chalcopyrite bioleached by *Leptospirillum ferriphilum* [J]. Electrochimica Acta, 2013, 103: 50−57.

[13] CÓRDOBA E M, MUÑOZ J A, BLÁZQUEZ M L, GONZÁLEZ F, BALLESTER A. Leaching of chalcopyrite with ferric ion. Part II: Effect of redox potential [J]. Hydrometallurgy, 2008, 93(3−4): 88−96.

[14] PAN Hao-dan, YANG Hong-ying, TONG Lin-lin, ZHONG Cong-bin, ZHAO Yu-shan. Control method of chalcopyrite passivation in bioleaching [J]. Transactions of Nonferrous Metals Society of China, 2012, 22(9): 2255−2260.

[15] KLAUBER C, PARKER A, van BRONSWIJK W, WATLING H. Sulphur speciation of leached chalcopyrite surfaces as determined by X-ray photoelectron spectroscopy [J]. International Journal of Mineral Processing, 2001, 62(1−4): 65−94.

[16] KLAUBER C. A critical review of the surface chemistry of acidic ferric sulphate dissolution of chalcopyrite with regards to hindered dissolution [J]. International Journal of Mineral Processing, 2008, 86(1−4): 1−17.

[17] SASAKI K, TAKATSUGI K, TUOVINEN O H. Spectroscopic analysis of the bioleaching of chalcopyrite by *Acidithiobacillus caldus* [J]. Hydrometallurgy, 2012, 127: 116−120.

[18] ACRES R G, HARMER S L, BEATTIE D A. Synchrotron XPS studies of solution exposed chalcopyrite, bornite, and heterogeneous chalcopyrite with bornite [J]. International Journal of Mineral Processing, 2010, 94(1−2): 43−51.

[19] PARKER A, KLAUBER C, KOUGIANOS A, WATLING H R, van BRONSWIJK W. An X-ray photoelectron spectroscopy study of the mechanism of oxidative dissolution of chalcopyrite [J]. Hydrometallurgy, 2003, 71(1−2): 265−276.

[20] GHAHREMANINEZHAD A, DIXON D G, ASSELIN E. Electrochemical and XPS analysis of chalcopyrite ($CuFeS_2$) dissolution in sulfuric acid solution [J]. Electrochimica Acta, 2013, 87: 97−112.

[21] ZHU Wei, XIA Jin-lan, YANG Yi, NIE Zhen-yuan, ZHENG Lei, MA Chen-yan, ZHANG Rui-yong, PENG An-an, TANG Lu, QIU Guan-zhou. Sulfur oxidation activities of pure and mixed thermophiles and sulfur speciation in bioleaching of chalcopyrite [J]. Bioresource Technology, 2011, 102(4): 3877−3882.

[22] HE Huan, XIA Jin-lan, YANG Yi, JIANG Hong-chen, XIAO Chun-qiao, ZHENG Lei, MA Chen-yan, ZHAO Yi-dong, QIU Guan-zhou. Sulfur speciation on the surface of chalcopyrite leached by *Acidianus manzaensis* [J]. Hydrometallurgy, 2009, 99(1−2): 45−50.

[23] HARMER S L, THOMAS J E, FORNASIERO D, GERSON A R. The evolution of surface layers formed during chalcopyrite leaching [J]. Geochimica et Cosmochimica Acta, 2006, 70(17): 4392−4402.

[24] NIE Zhen-yuan, GU Guo-hua, YANG Hui-sha, QIU Guan-zhou. Bioleaching of pyrrhotite by *Sulfobacillus thermosulfidooxidans* [J]. Journal of Central South University, 2014, 21(7): 2638−2644.

[25] QIN Wen-qing, ZHEN Shi-jie, YAN Zhong-qiang, CAMPBELL Maurice, WANG Jun, LIU Kai, ZHANG Yan-sheng. Heap bioleaching of a low-grade nickel-bearing sulfide ore containing high levels of magnesium as olivine, chlorite and antigorite [J]. Hydrometallurgy, 2009, 98(1−2): 58−65.

[26] YANG Cong-ren, QIN Wen-qing, LAI Shao-shi, WANG Jun, ZHANG Yan-sheng, JIAO Fen, REN Liu-yi, ZHUANG Tian, CHANG Zi-yong. Bioleaching of a low grade nickel–copper–cobalt sulfide ore [J]. Hydrometallurgy, 2011, 106(1−2): 32−37.

[27] HIROYOSHI N, MIKI H, HIRAJIMA T, TSUNEKAWA M. Enhancement of chalcopyrite leaching by ferrous ions in acidic ferric sulfate solutions [J]. Hydrometallurgy, 2001, 60(3): 185−197.

[28] SANDSTRÖM Å, SHCHUKAREV A, PAUL J. XPS characterisation of chalcopyrite chemically and bio-leached at high and low redox potential [J]. Minerals Engineering, 2005, 18(5): 505−515.

[29] ARCE E M, GONZ LEZ I. A comparative study of electrochemical behavior of chalcopyrite, chalcocite and bornite in sulfuric acid solution [J]. International Journal of Mineral Processing, 2002, 67(1−4): 17−28.

[30] VELASQUEZ P, LEINEN D, PASCUAL J, RAMOS-BARRADO J R, GREZ P, GOMEZ H, SCHREBLER R, del RIO R, CÓRDOVA R. A chemical, morphological, and electrochemical (XPS, SEM/EDX, CV, and EIS) analysis of electrochemically modified electrode surfaces of natural chalcopyrite ($CuFeS_2$) and pyrite (FeS2) in alkaline solutions [J]. Journal of Physical Chemistry B, 2005, 109(11): 4977−4988.

[31] VILCÁEZ J, SUTO K, INOUE C. Bioleaching of chalcopyrite with thermophiles: Temperature–pH–ORP dependence [J]. International Journal of Mineral Processing, 2008, 88(1−2): 37−44.

[32] VILCÁEZ J, YAMADA R, INOUE C. Effect of pH reduction and ferric ion addition on the leaching of chalcopyrite at thermophilic temperatures [J]. Hydrometallurgy, 2009, 96(1−2): 62−71.

[33] NAVA D, GONZALEZ I, LEINEN D, RAMOS-BARRADO J R. Surface characterization by X-ray photoelectron spectroscopy and cyclic voltammetry of products formed during the potentiostatic reduction of chalcopyrite [J]. Electrochimica Acta, 2008, 53(14): 4889−4899.

[34] KLAUBER C. Fracture-induced reconstruction of a chalcopyrite ($CuFeS_2$) surface [J]. Surface and Interface Analysis, 2003, 35(5): 415−428.

[35] ACRES R G, HARMER S L, BEATTIE D A. Synchrotron XPS, NEXAFS, and ToF-SIMS studies of solution exposed chalcopyrite and heterogeneous chalcopyrite with pyrite [J]. Minerals Engineering, 2010, 23(11−13): 928−936.

[36] de OLIVEIRA C, DUARTE H A. Disulphide and metal sulphide formation on the reconstructed (001) surface of chalcopyrite: A DFT study [J]. Applications of Surface Science, 2010, 257(4): 1319−1324.

[37] GOH S W, BUCKLEY A N, LAMB R N, ROSENBERG R A, MORAN D. The oxidation states of copper and iron in mineral sulfides, and the oxides formed on initial exposure of chalcopyrite and bornite to air [J]. Geochimica et Cosmochimica Acta, 2006, 70(9): 2210−2228.

[38] LI J, KAWASHIMA N, KAPLUN K, ABSOLON V J, GERSON A R. Chalcopyrite leaching: The rate controlling factors [J]. Geochimica et Cosmochimica Acta, 2010, 74(10): 2881−2893.

[39] GERSON A R, BREDOW T. Interpretation of sulphur 2p XPS spectra in sulfide minerals by means ofab initio calculations [J]. Surface and Interface Analysis, 2000, 29(2): 145−150.

[40] SMART R S, SKINNER W M, GERSON A R. XPS of sulphide mineral surfaces: Metal-deficient, polysulphides, defects and elemental sulphur [J]. Surface and Interface Analysis, 1999, 28(1): 101−105.

[41] YIN Q, KELSALL G H, VAUGHAN D J, ENGLAND K E R. Atmospheric and electrochemical oxidation of the surface of chalcopyrite ($CuFeS_2$) [J]. Geochimica et Cosmochimica Acta, 1995, 59(6): 1091−1100.

[42] BRION D. Study by photoelectron-spectroscopy of surface degradation of FeS_2, $CuFeS_2$, ZnS and PbS exposed to air and water [J]. Applications of Surface Science, 1980, 5(2): 133−152. (in French)

[43] YIN M, WU C K, LOU Y B, BURDA C, KOBERSTEIN J T, ZHU Y M, O'BRIEN S. Copper oxide nanocrystals [J]. Journal of the American Chemical Society, 2005, 127(26): 9506−9511.

[44] CHUSUEI C C, BROOKSHIER M A, GOODMAN D W. Correlation of relative X-ray photoelectron spectroscopy shake-up intensity with CuO particle size [J]. Langmuir, 1999, 15(8): 2806−2808.

[45] EGHBALNIA M, DIXON D G. Electrochemical study of leached chalcopyrite using solid paraffin-based carbon paste electrodes [J]. Hydrometallurgy, 2011, 110(1−4): 1−12.

[46] LIANG Chang-li, XIA Jin-lan, YANG Yi, NIE Zhen-yuan, ZHAO Xiao-juan, ZHENG Lei, MA Chen-yan, ZHAO Yi-dong. Characterization of the thermo-reduction process of chalcopyrite at 65 °C by cyclic voltammetry and XANES spectroscopy [J]. Hydrometallurgy, 2011, 107(1−2): 13−21.

[47] GÓMEZ C, FIGUEROA M, MUÑOZ J, BLÁZQUEZ M L, BALLESTER A. Electrochemistry of chalcopyrite [J]. Hydrometallurgy, 1996, 43(1−3): 331−344.

[48] LÓPEZ-JUÁREZ A, GUTIÉRREZ-ARENAS N, RIVERA-SANTILLÁN R E. Electrochemical behavior of massive chalcopyrite bioleached electrodes in presence of silver at 35 °C [J]. Hydrometallurgy, 2006, 83(1−4): 63−68.

[49] D'HUGUES P, FOUCHER S, GALLE-CAVALLONI P, MORIN D. Continuous bioleaching of chalcopyrite using a novel extremely thermophilic mixed culture [J]. International Journal of Mineral Processing, 2002, 66(1−4): 107−119.

[50] MAJUSTE D, CIMINELLI V S T, OSSEO-ASARE K, DANTAS M S S, MAGALHAES-PANIAGO R. Electrochemical dissolution of chalcopyrite: Detection of bornite by synchrotron small angle X-ray diffraction and its correlation with the hindered dissolution process [J]. Hydrometallurgy, 2012, 111: 114−123.

黄铜矿在 50 °C 浸出过程中表面硫组成

吴世发，杨聪仁，覃文庆，焦 芬，王 军，张雁生

中南大学 资源加工与生物工程学院，长沙 410083

摘 要：利用 X-射线光电子能谱(XPS)和循环伏安(CV)法研究黄铜矿的钝化膜组成。浸出试验结果表明：无菌浸出和微生物浸出黄铜矿 30 d 后，Cu 的浸出率分别为 4.0%和 21.5%，Fe 的浸出率分别为 3.8%和 10.5%。XPS 分析结果表明：黄铜矿经无菌浸出和微生物浸出后，黄铜矿晶格的中 Fe 原子优先溶解到溶液中，并且在其表面形成 S_2^{2-}、S_n^{2-}和 S^0。此外，黄铜矿经微生物浸出后，其表面还检测到 SO_4^{2-}，并且认为 SO_4^{2-}是以黄钾铁矾的形式存在。CV 研究结果表明：$Cu_{1-x}Fe_{1-y}S_{2-z}$($y>x$)和 S^0 导致黄铜矿电极表面钝化。元素硫和黄钾铁矾包裹在黄铜矿表面对其浸出有一定的影响，然而二硫化物、多硫化物或者缺金属硫化物对阻碍黄铜矿浸出起更关键的作用。

关键词：生物浸出；黄铜矿；钝化膜；电化学

(Edited by Mu-lan QIN)